An improved zero vibration method and parameter sensitivity analysis for the swing control of bridge-type grab ship unloader

Zhou, Y; Zhang, X.; Yu, Z; Schott, DL; Lodewijks, G

DOI
10.1177/0954406215597957

Publication date
2016

Document Version
Final published version

Published in
Institution of Mechanical Engineers. Proceedings. Part C: Journal of Mechanical Engineering Science

Citation (APA)
Zhou, Y., Zhang, X., Yu, Z., Schott, DL., & Lodewijks, G. (2016). An improved zero vibration method and parameter sensitivity analysis for the swing control of bridge-type grab ship unloader. *Institution of Mechanical Engineers. Proceedings. Part C: Journal of Mechanical Engineering Science*, *230*(14), 2463-2472. https://doi.org/10.1177/0954406215597957

Original Article

Institution of MECHANICAL ENGINEERS
Journal of MECHANICAL ENGINEERING SCIENCE

Proc IMechE Part C:
J Mechanical Engineering Science
2016, Vol. 230(14) 2463–2472

DOI: 10.1177/0954406215597957
pic.sagepub.com
SAGE

An improved zero vibration method and parameter sensitivity analysis for the swing control of bridge-type grab ship unloader

Yong Zhou[1,2], Xinyuan Zhang[1], Zhenzhen Yu[1], Dingena Schott[2] and Gabriel Lodewijks[1,2]

Abstract

This paper presents an improved zero vibration method for the swing control of bridge-type grab ship unloader. With the method, the concepts of equivalent frequency and the equivalent damping ratio are proposed to cope with the changeable length of rope, and the optimal path planning is considered to avoid collision and improve efficiency. Numerical simulation results of a case study indicate that the maximum residual swing angle of the grab can be limited to a small range to ensure safety using the improved zero vibration method, whereas the traditional zero vibration method with average frequency and zero damping ratio gets poor results of swing control. After that, the sensitivities of the max residual swing angle to the changes of some main design parameters (damping coefficient, deviation of the center of gravity of the grab in rope direction, and time delay of the system) and operating parameters (position deviation of the trolley, initial length deviation of the rope, and initial swing angle) are analyzed. The results obtained display that the residual swing angle is sensitive to the deviation of grab's center of gravity, the deviation of trolley's position, and the initial swing angle under the same control parameters, but insensitive to the damping coefficient, the time delay of the system, and the initial length deviation of the rope. This can help to select the appropriate parameter values or adaptive range in an actual unloader.

Keywords

Grab ship unloader, improved zero vibration method, parameter sensitivity analysis, swing control

Date received: 4 November 2014; accepted: 6 July 2015

Introduction

Input-shaping methods are an important part of theory and application for the control of flexible dynamic systems. The major advantage of the methods is that they do not require sensors, although sensors can be used sometimes to improve performance. Another strength of input shaping is that it acts to suppress vibration in a feedforward way that is faster than anything possible with feedback control.[1]

Cranes that use cables to lift and transport the payload are typical flexible dynamic systems. The residual oscillation of the payload could affect the work efficiency and even the safety. Many researchers have devoted their efforts to the research of input-shaping techniques on cranes. Singer et al.[2] presented a fixed duration shapers to reduce residual oscillations of gantry cranes. Singhose et al.[3,4] evaluated several versions of input shapers and compared them with time-optimal rigid-body commands over a wide range of parameters for the control of planar gantry cranes. Hong et al.[5] investigated a modified command shaping control to reduce residual vibrations at a target position and to limit the sway angle of the payload during traveling of the trolley of the container cranes. Blackburn et al.[6,7] proposed a novel command shaping algorithm for reducing vibration for the nonlinear slewing motions of the tower crane. Khalid et al.[8] studied the performance of human operators using input-shaping controller on a large bridge crane. Ngo et al.[9] investigated a combination of command shaping and bang/off-bang control scheme for container cranes. Veciana and Cardona defined the

[1]School of Logistics Engineering, Wuhan University of Technology, Wuhan, China
[2]Section of Transport Engineering and Logistics, Delft University of Technology, Delft, The Netherlands

Corresponding author:
Yong Zhou, School of Logistics Engineering, Wuhan University of Technology, Wuhan 430063, China.
Email: zhouyong@whut.edu.cn

motion profiles through convolution of pulses multiplied by a negative exponential time function considering damping[10,11] and developed an approach to design command inputs for the reduction of residual vibrations in nonzero initial states for cranes.[12]

Some researchers combined feedback or adaptive control with input-shaping method to control the swing of crane. Sorensen et al.[13] developed a control scheme to enable precise positioning of a crane payload, where feedback control was used for positioning and disturbance rejection, and input shaping was used for motion-induced sway reduction. Stergiopoulos and Tzes[14] presented an adaptive input-shaping technique to suppress the payload oscillations on a three-dimensional overhead crane with hoisting mechanism, where the simplified linear models were considered as a time-varying linear system. Garrido et al.[15] achieved the antiswing control of an automatic overhead crane using the online two-dimensional inclinometer measurements and an online calculation of input impulse trains.

The input-shaping methods based on double pendulum model of crane have also been developed. Singhose et al.[16–18] built a double pendulum model for bridge crane and designed the input-shaping controller to suppress the multimode vibration. Vaughan et al.[19] proposed an input shaper method to improve the ability of crane operators to drive a double-pendulum tower crane. Masoud et al.[20,21] designed a hybrid command-shaper to generate acceleration commands to suppress travel and residual oscillations of a double-pendulum overhead crane.

Zero vibration (ZV) shaper is the classic input-shaping method that was presented in the 1950s.[22] It is excellent to depress residual vibration when the frequency and damping ratio of flexible dynamic system are unchangeable. However, traditional ZV (TZV) shaper is sensitive to modeling errors and is not adaptive for the system of varying frequency and damping ratio. Some robust methods were proposed, such as zero vibration and derivative (ZVD) shaper[23] and extra-insensitive shapers.[24] The specified-insensitivity input-shaping method was also developed to deal with the modeling errors, in which a specified level of robustness was defined to design the input shapers.[25] Unfortunately, robust shapers typically have longer durations that slow the system response.[26–28] For example, the ZVD shaper takes longer than the ZV shaper by one half period of the vibration, which is a small influence for the most high frequency system. However, for large crane equipment that usually operates with large rope lengths, the increase of one half period of the oscillation might affect transportation efficiency severely. In addition, some adaptive technology could be used on line difficultly because of the limitation of the controllers' calculating capacity for most of the cranes.

Negative input shapers that contain negative impulses can give much faster rise time than positive input shapers.[29] However, the negative impulses may result in a small cost of robustness and possible high mode excitation that need be dealt with using appropriate strategies.[30–32]

An improved ZV (IZV) method for bridge-type grab ship unloader is presented in this paper. The method uses the equivalent frequency and equivalent damping ratio to respond to system changes in rope length, which can control the residual swing angle in a certain range. Because the output shafts of the trolley drive motor and the hoisting motor in modern unloader are usually equipped with high-resolution rotary encoders, the exact location of the trolley and actual length of the rope can be acquired precisely. Therefore, the modeling error can be controlled within a small range. In order to analyze the influence of parameters errors on the control effect, this paper also presents the sensitivity analysis of major designing and operating parameters.

This paper is organized as follows. In the next section, a dynamic model of trolley–grab system is established, where the system damping is considered. An IZV shaper and path planning method are proposed in the subsequent section. A case study is presented in the following section, in which the simulation of swing control is achieved and parameter sensitivity is discussed. In the final section, conclusions and future perspectives are presented.

Dynamic model of trolley–grab system

Many literatures have built a dynamic model of trolley–payload system. However, some of the literatures did not consider the changes of the rope,[13,33,34] and some others did not consider damping.[3,4,9,35] Here, a dynamic model of trolley–grab system is built with these following assumptions:

1. The trolley and the grab move in the same plane.
2. The grab is considered as a mass point.
3. The damping of the air is considered as the linear damping which acts on the motion direction of the grab.
4. The elastic deformations of the rope, influence of wind, as well as the frictions between the rope and the pulleys are neglected.

Take the position of the center of gravity of the trolley as the coordinate origin O_1 (x_M, y_M) and build the inertial coordinate system O_1–XY, where the directions of X and Y are level and vertical directions, respectively. Then, the dynamic model of the trolley–grab system can be built as shown in Figure 1, in which, $O_2(x_m, y_m)$ is the coordinate of the grab; M and m are the masses of the trolley and the grab, respectively; F, f, and F_l are the drive force, friction on the trolley, and the pull force of the rope, respectively; l and θ are the length of the rope and the swing angle of the grab, respectively; c is the damping coefficient.

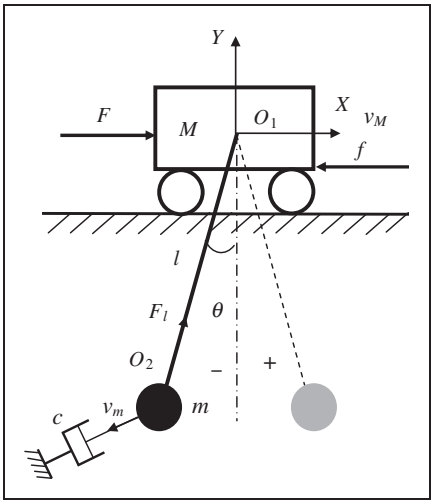

Figure 1. Dynamic model of the trolley–grab system.

According to Figure 1, the trolley–grab system can be defined by three generalized coordinates that are the displacement of trolley x, swing angle of the grab θ, and the length of the rope l. Then, in terms of the geometric relationship, one can get

$$\begin{cases} x_M = x \\ y_M = 0 \\ x_m = x + l\sin\theta \\ y_m = -l\cos\theta \end{cases} \tag{1}$$

Then the velocity components of the trolley and the grab are

$$\begin{cases} \dot{x}_M = \dot{x} \\ \dot{y}_M = 0 \\ \dot{x}_m = \dot{x} + \dot{l}\sin\theta + l\dot{\theta}\cos\theta \\ \dot{y}_m = -\dot{l}\cos\theta + l\dot{\theta}\sin\theta \end{cases} \tag{2}$$

Let the velocity of the trolley be v_M, and the velocity of the grab be v_m, then, the kinetic energy of the system can be expressed by

$$T = \frac{1}{2}Mv_M^2 + \frac{1}{2}mv_m^2 \tag{3}$$

where

$$\begin{cases} v_M = \dot{x}_M \\ v_m = \sqrt{\dot{x}_m^2 + \dot{y}_m^2} \end{cases} \tag{4}$$

Substituting equation (4) and equation (2) into equation (3) results in

$$\begin{aligned} T = {} & \frac{1}{2}(M+m)\dot{x}^2 + \frac{1}{2}m(\dot{l}^2 + l^2\dot{\theta}^2) \\ & + m\dot{x}(\dot{l}\sin\theta + l\dot{\theta}\cos\theta) \end{aligned} \tag{5}$$

Take height of O_1 as the zero potential energy level, thus the potential energy of the system can be expressed by

$$V = -mgl\cos\theta \tag{6}$$

Let dissipation function be G, then

$$G = \frac{1}{2}c(\dot{x}_m^2 + \dot{y}_m^2) \tag{7}$$

Substituting equation (2) into equation results in

$$G = \frac{1}{2}c\left(\dot{x}^2 + \dot{l}^2 + l^2\dot{\theta}^2 + 2\dot{x}\dot{l}\sin\theta + 2\dot{x}l\dot{\theta}\cos\theta\right) \tag{8}$$

Using the Lagrange method, one can get the system dynamic equation as follows

$$\frac{d}{dt}\left(\frac{\partial L}{\partial \dot{q}_i}\right) - \frac{\partial L}{\partial q_i} + \frac{\partial G}{\partial \dot{q}_i} = F_i \tag{9}$$

where L is the Lagrange function, while $L = T - U$; q_i is the generalized coordinate, while $q_1 = x$, $q_2 = l$, $q_3 = \theta$; and F_j is the generalized force in terms of the generalized coordinate system, while $F_1 = F - f$, $F_2 = -F_l$, $F_3 = 0$. Then, one can get the motion differential equation of the system

$$\begin{cases} (M+m)\ddot{x} + m\ddot{l}\sin\theta + 2m\dot{l}\dot{\theta}\cos\theta + ml\ddot{\theta}\cos\theta \\ -ml\dot{\theta}^2\sin\theta + c\left(\dot{x} + \dot{l}\sin\theta + l\dot{\theta}\cos\theta\right) = F - f \\ m\ddot{l} + m\ddot{x}\sin\theta - ml\dot{\theta}^2 - mg\cos\theta \\ +c\left(\dot{l} + \dot{x}\sin\theta\right) = -F_l \\ 2m\dot{l}\dot{\theta} + ml\ddot{\theta} + m\ddot{x}\cos\theta + mg\sin\theta \\ +c\left(l\dot{\theta} + \dot{x}\cos\theta\right) = 0 \end{cases} \tag{10}$$

Because in the real control system the velocities $\dot{x}$ and $\dot{l}$ can be used as command input parameters, the acceleration $\ddot{x}$ can be derived from by $\dot{x}$, then the swing angle θ can be calculated by

$$2m\dot{l}\dot{\theta} + ml\ddot{\theta} + m\ddot{x}\cos\theta + mg\sin\theta + c(l\dot{\theta} + \dot{x}\cos\theta) = 0 \tag{11}$$

If the damping were not considered, the equation would be the same one exhibiting in some existing literatures.[4,9,33]

IZV shaper and path planning

IZV shaper

Assuming that the system is a second-order harmonic oscillator with natural frequency ω and damping ratio ζ, the constraint on residual vibration amplitude can be expressed as the ratio of residual vibration

amplitude of the response system with shaping to that without shaping. And it can be formulated as[2]

$$V(\omega,\zeta) = e^{-\zeta\omega t_n}\sqrt{[C(\omega,\zeta)]^2+[S(\omega,\zeta)]^2} \tag{12}$$

where

$$C(\omega,\zeta)=\sum_{i=1}^{n} A_i e^{\zeta\omega t_i}\cos(\omega\sqrt{1-\zeta^2}t_i) \tag{13}$$

$$S(\omega,\zeta)=\sum_{i=1}^{n} A_i e^{\zeta\omega t_i}\sin(\omega\sqrt{1-\zeta^2}t_i) \tag{14}$$

in which A_i and t_i are the amplitudes and time locations of the impulses, respectively.

To design a TZV shaper, one can take $n=2$ and have[22,23]

$$\begin{cases} V(\omega,\zeta) == 0 \\ A_1+A_2=1 \\ t_1=0 \end{cases} \tag{15}$$

Then, one can get

$$\begin{cases} A_1=\frac{1}{1+K} \\ A_2=\frac{K}{1+K} \\ t_1=0 \\ t_2=\frac{\pi}{\omega\sqrt{1-\zeta^2}} \end{cases} \tag{16}$$

where

$$K = e^{-\zeta\pi/\sqrt{1-\zeta^2}} \tag{17}$$

For the system with a fixed rope length ($\dot{l}=0$), the ω and the ζ are constants (equations (19) and (20)). However, in order to improve the efficiency, the grab should be lifted or lowered when the trolley is moving.

Assuming that the swing angle of the payload is small, $\sin\theta\approx\theta$ $\cos\theta\approx 1$. Thus, equation (11) can be simplified as

$$\ddot{\theta}+\frac{\left(2m\dot{l}+cl\right)}{ml}\dot{\theta}+\frac{g}{l}\theta+\frac{m\ddot{x}+c\dot{x}}{ml}=0 \tag{18}$$

Considering that the $\dot{x}$, $\dot{l}$, and l can be used as known parameters, equation (18) can be looked as a second-order oscillation process with time-varying parameters around the swing angle θ, and its natural frequency and damping ratio can be calculated by

$$\omega=\sqrt{\frac{g}{l}} \tag{19}$$

$$\zeta=\frac{\dot{l}}{\sqrt{gl}}+\frac{c}{2m}\sqrt{\frac{l}{g}} \tag{20}$$

Apparently, the nature frequency and the damping ratio will vary with the length of the rope. Input shapers designed with the average operating frequency are more effective than shapers based on the initial frequency.[3,4] However, average frequency usually could not achieve an optimal swing control effect. In addition, the changes in damping ratio cannot be ignored. Here, the concepts of equivalent frequency ω_e and equivalent damping ratio ζ_e are proposed, then, one can get

$$\omega_{\min}\leqslant\omega_e\leqslant\omega_{\max} \tag{21}$$

$$\zeta_{\min}\leqslant\zeta_e\leqslant\zeta_{\max} \tag{22}$$

where $\omega_{\min}$, $\omega_{\max}$, $\zeta_{\min}$, and $\zeta_{\max}$ are minimal frequency, maximal frequency, minimal damping ratio, and maximal damping ratio, respectively. Their values are decided by l and $\dot{l}$ according to equations (19) and (20).

Here, the fourth-order Runge–Kutta method is used to calculate the response of the system according to equation (11). Comparing with the TZV methods involving fixed rope length or average frequency, the improvement obtained by equivalent frequency and equivalent damping ratio can control the residual swing angle in a small range and varying cable length can be considered. The IZV shaper design algorithm can be summarized as follows:

1. Select a desired limit value on the residual swing angle θ_l and calculate minimal frequency, maximal frequency, minimal damping ratio, and maximal damping ratio.
2. Design ZV shaper according to frequency ω_c and damping ratio ζ_c and calculate the residual swing angle θ_r in terms of equation (11), in which $\omega_c=\omega_{\min}$, $\zeta_c=\zeta_{\min}$.
3. Take frequency increment $\Delta\omega$ and damping ratio increment $\Delta\zeta$. Start at step 2 and replace ω_c with $\omega_c+\Delta\ \omega$ and ζ_c with $\zeta_c+\Delta\zeta$ until $\omega_c+\Delta\omega>\omega_{\max}$ and $\zeta_c+\Delta\zeta>\zeta_{\max}$.
4. Compare all the residual swing angles that are calculated by step 2 and 3, and select the minimal one as $\theta_{r\min}$.
5. If $\theta_{r\min}<\theta_l$, the corresponding frequency ω_c and damping ratio ζ_c are regarded as equivalent frequency ω_e and equivalent damping ratio ζ_e, respectively.

The search algorithm is time consuming relatively, and further research may consider faster optimization technique, such as GA and improved initial guess.[36]

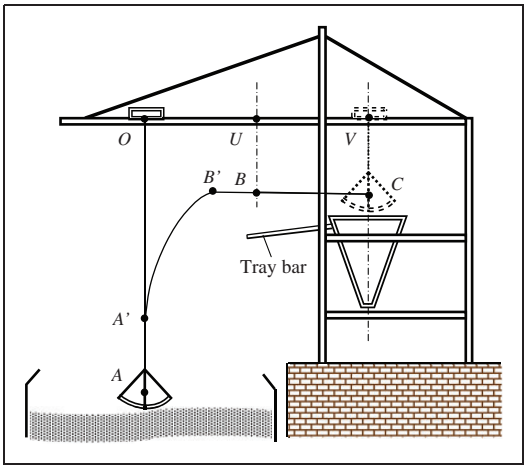

Figure 2. Travel path of grab ship unloader.

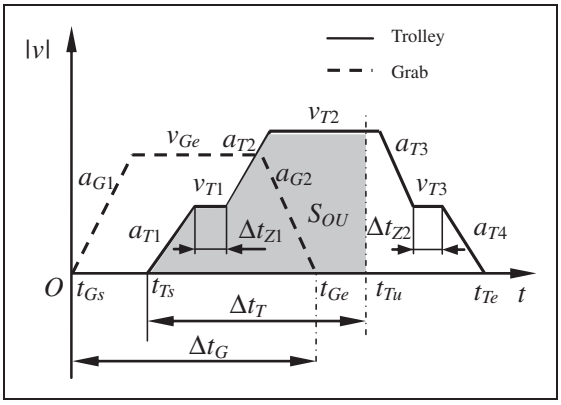

Figure 3. Sketch map of the speed curves of the grab and the trolley.

Path planning

When a ship unloader is operating, on the one hand, the grab should be lifted or lowered while the trolley is moving to improve the efficiency, on the other hand collision should be avoided. Therefore, the travel path of the trolley and the grab should be planned advisably. As shown in Figure 2, the point B is a critical point that is provided by the manufacturer to avoid collision, which means that the grab should be lifted to the highest position in rope direction before the trolley arrives at point U. The full load travel of the grab (A to C) will be explained as an example here and a similar method can be used in the empty load travel of the grab (C to A). When the point B is determined by the manufacturer, the swing of the grab is considered to avoid possible collision and thus it is not necessary to consider the swing in the path planning. Furthermore, since only the speed of the trolley is shaped using input-shaping method, lifting of the grab can operate in accordance with the rated velocity and acceleration. Obviously, in order to avoid collisions and ensure efficiency, lifting of the grab can run prior to or simultaneously with the running of the trolley. In Figure 2, the grab will move along the path of $A \rightarrow A' \rightarrow B' \rightarrow B \rightarrow C$. If hoisting of the grab and moving of the trolley begin simultaneously, the points A and A' will coincide. Meanwhile, if the trolley reaches the point U and the grab reaches the point B at the same time, the point B and B' will coincide.

As shown in Figure 3, the dashed line is the lift velocity of the grab along the rope direction, and the solid line is the velocity curve of the trolley generated with ZV shaping. Here, t_{Gs} and t_{Ge} are the start time and end time of lifting of the grab, respectively; t_{Ts} and t_{Te} are the start time and end time of moving of the trolley, respectively; t_{Tu} and S_{OU} (the shaded area) are the time when the trolley reaches the point U and the distance between point O and point U, respectively.

The time constraint of lifting of the grab is given by

$$t_{Gs} = 0 \tag{23}$$

The total time of lifting Δt_G can be solved according to the changing length of the rope Δl, rated lift speed v_{Ge}, and rated up/down acceleration a_{G1}/a_{G2}

$$\Delta t_G = f(\Delta l, a_{Gu}, a_{G1}, v_{G2}) \tag{24}$$

The time constraints of moving of the trolley are given by

$$\begin{cases} t_{Ts} \geqslant 0 \\ t_{Tu} \geqslant t_{Ge} \end{cases} \tag{25}$$

The time of moving of the trolley from point O to point U Δt_G can be solved in terms of shaped speed curve of the trolley

$$\begin{aligned} \Delta t_T = g(&S_{OU}, v_{T1}, v_{T2}, v_{T3}, a_{T1}, a_{T2}, \\ &a_{T3}, a_{T4}, \Delta t_{Z1}, \Delta t_{Z2}) \end{aligned} \tag{26}$$

In which, v_{Ti}, a_{Tj}, and Δt_{Zk} ($i=3$, $j=4$, $k=2$) are the velocities, accelerations, and delay times of different stages in shaped speed curve of the trolley, respectively.

If $\Delta t_T \geqslant \Delta t_G$, let $t_{TS} = 0$; if $\Delta t_T < \Delta t_G$, let $t_{Tu} = t_{Ge}$. Then, the total running time t_{TE} can be got to a minimum under the constraint conditions of equation (25).

Case study

Some results of the numerical analysis proposed in previous section are displayed in this section. Table 1 lists the main parameters of a bridge-type grab ship unloader in the case study.

Table 1. Main parameters of an 800 t/h grab ship unloader from Jiujiang Coal Terminal of China.

Parameter	Value	
	Full load	Empty load
Acceleration/deceleration of lift (m/s^2)	0.67	0.67
Rated velocity of lift (m/s)	2.0	2.0
Acceleration/deceleration of trolley (m/s^2)	0.72	0.72
Rated velocity of trolley (m/s)	2.16	2.16
Mass of grab (t)	8	
Maximal payload (t)	12	
Range of trolley travel (m)	9–23	
Range of rope length (m)	7–46	
Safe distance to avoid collision (m)(from *U* to *V* in Figure 2)	8.5	

Simulation of ZV shaper control

The simulation takes a typical work status of the unloader, travel of the trolley $S = 21$ m, and the initial length of the rope $l = 25$ m. In addition, let unloading time be 5 s, system time delay be 0 ms, damping coefficient be 20 N/(m/s), and initial swing angle be 0°. From Figure 2, the path of the grab in a work cycle is $A \rightarrow B \rightarrow C \rightarrow B \rightarrow A$, in which $A \rightarrow B \rightarrow C$ is the full load path and $C \rightarrow B \rightarrow A$ is the back path with empty load. Using the method presented in this paper, one can get the equivalent frequency of full load $\omega_{ef} = 0.9614$ rad/s, the equivalent damping ratio of full load $\zeta_{ef} = -0.1122$, the equivalent frequency of empty load $\omega_{ee} = 0.9614$ rad/s, and the equivalent damping ratio of empty load $\zeta_{ee} = 0.1119$, respectively. It should be noted that, although the damping ratio of the full load has a negative value here, the system will not behave unsteadily because the rules for what a negative damping ratio mean on a linear system do not strictly apply when the damping ratio concept is used on a nonlinear system.

Figure 4 shows the command speed curves of the trolley and the grab corresponding to IZV method and TZV method, in which the speed of the grab is only in the direction of the rope. In the TZV method, the frequencies of full load and empty load are both taken as the average frequency 0.9047 rad/s and the damp ratios are both taken as zero. According to Figure 4, one can find that the max speeds of the trolley and the grab lifting are both achieved at the rated velocities. In order to avoid collision, the grab has to be lifted first, and then the trolley starts to ensure the efficiency. Mainly there are some differences in the speed curves of the trolley between IZV method and TZV method. Moreover, because there

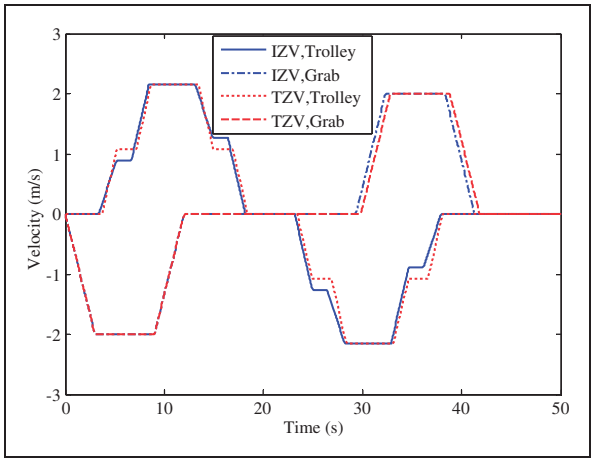

Figure 4. Command speed curves of the trolley and the grab.

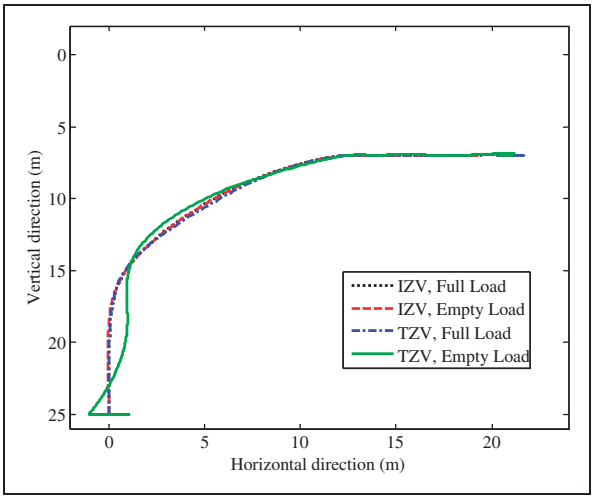

Figure 5. Travel track of the grab in a work cycle.

are negative damping ratios in IZV method, the larger second impulse amplitudes are obtained in the shaper.

Figure 5 shows the travel track of the grab in a work cycle, and the swing angle of the grab varying with the time is shown in Figure 6.

The results as shown in Figures 5 and 6 exhibit that a good effect of swing control is obtained using the IZV method, in which the max residual swing angle in the full load travel is 0.3° ($t = 20.6$ s) and the max residual swing angle in the empty load travel is 0.06° ($t = 42.6$ s). Whereas, using the TZV method, the max residual swing angle in the full load travel is 5.9° ($t = 20.5$ s) and the max residual swing angle in the empty load travel is 2.4° ($t = 41.8$ s).

Parameter sensitivity analysis

Because the simulation analysis is based on a model of the real ship unloader, the sensitivities of the max residual swing angle to the changes of some main designing parameters and operating parameters

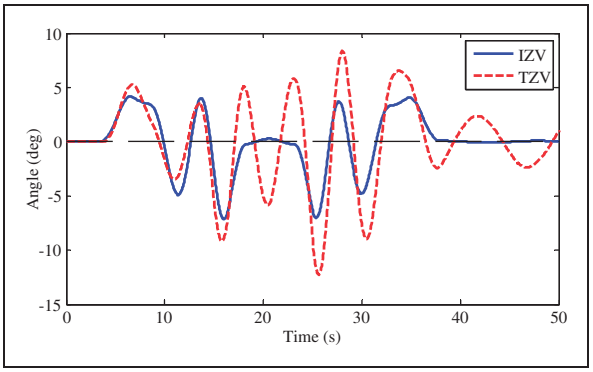

Figure 6. Swing angle of the grab varying with the time.

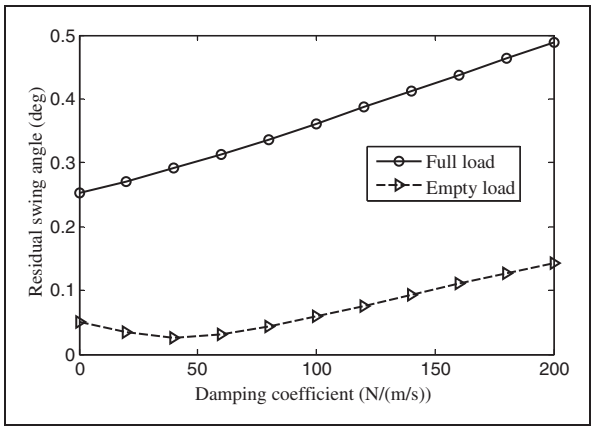

Figure 7. Curves of the residual swing angle varying with the damping coefficient.

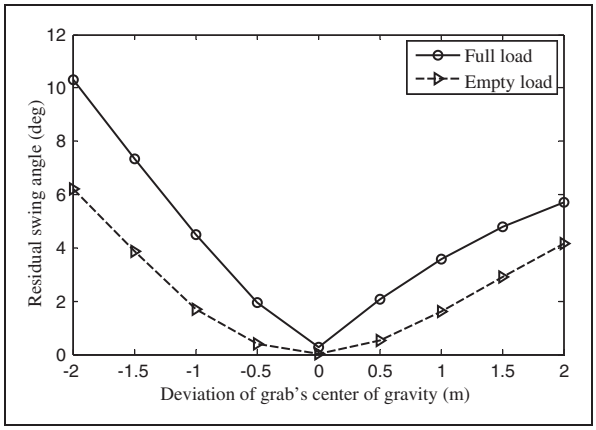

Figure 8. Curves of the residual swing angle varying with the deviation of the center of gravity of the grab in rope direction.

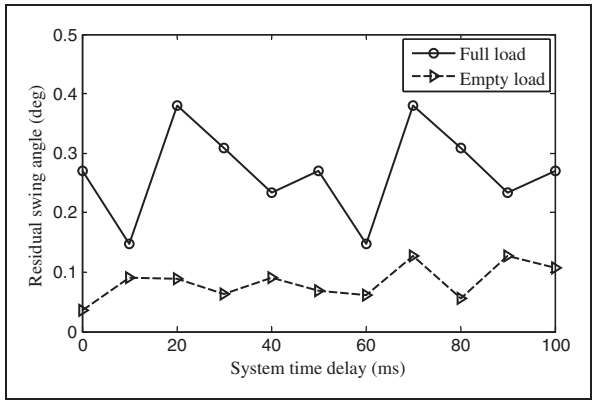

Figure 9. Curves of the residual swing angle varying with the time delay of the system.

should be analyzed. The insensitive parameters can be ignored or given approximate values and the sensitive parameters need be given accurate values or applicable ranges. Here, the control parameters that are derived from "Simulation of ZV shaper control" section are used as basic control parameters in the sensitivity analysis.

First, the possible errors of several designing parameters are considered. Since it is often difficult to obtain the accurate value of damping coefficient, a wide range is given here to analyze its impact. In fact, the literatures have given very different values.[34,37] Figures 7 to 9 show the curves of the residual swing angle changing with the damping coefficient, the deviation of the center of gravity of the grab in rope direction, and the time delay of the system, respectively.

In Figure 7, the residual swing angles of full load path vary in the range of (0.25°, 0.49°), that of empty load path in the range of (0.026°, 0.14°) when the damping coefficient varies in the range of (0 N/(m/s), 200 N/(m/s)), which indicates that the residual swing angle is insensitive to the damping coefficient. In Figure 8, the residual swing angles increase with the increasing deviation of grab's center of gravity. The residual swing angles of full load path and empty load path reach 10.29° and 6.21°, respectively, when the deviation of grab's center of gravity is −2 m. Therefore, the position of grab's center of gravity should be as accurate as possible. Obviously, when a grab loads and opens, the center of gravity may change. Then full load and empty load path should differ from the center of gravity of the grab. Figure 9 shows that the time delay of the system has little effect on the residual swing angle and the effect has no obvious pattern. Therefore, the parameter can be ignored.

Second, several operating parameters are selected to analyze the favorable working conditions of the control parameters. Figure 10 illustrates the characteristics of the residual swing angles varying with position deviation of the trolley and initial length deviation of the rope, and Figure 11 shows the curves of the residual swing angle varying with the initial swing angle.

From Figure 10, one can find that the residual swing angle is sensitive to the varying initial position of the trolley but it is insensitive to the varying initial length of the rope, which illustrates that same group

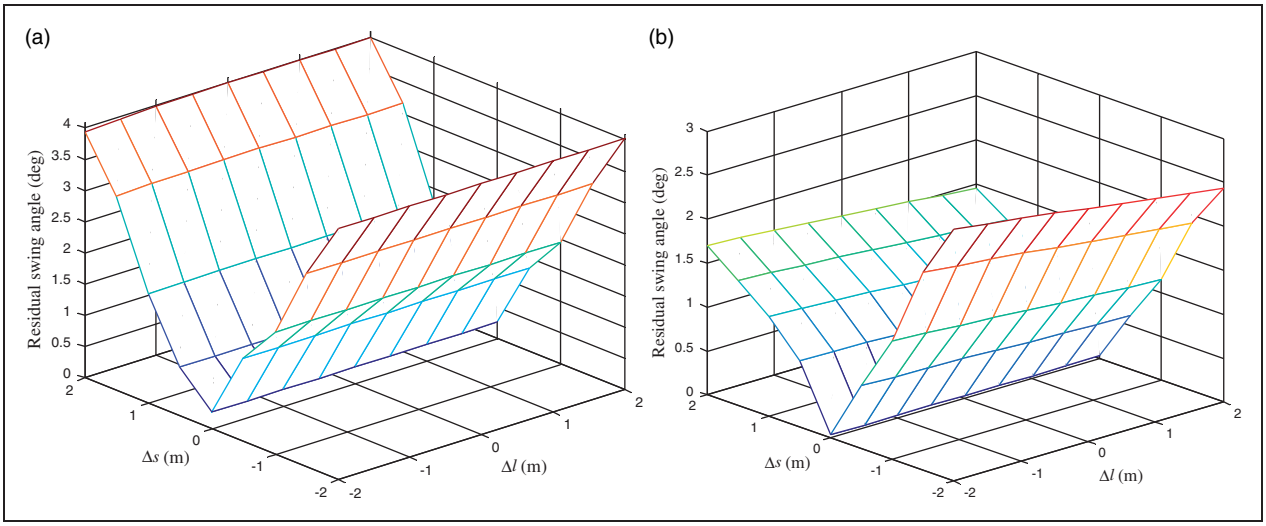

Figure 10. Characteristics of the residual swing angles varying with position deviation of the trolley and initial length deviation of the rope. (a) Full load, (b) empty load.

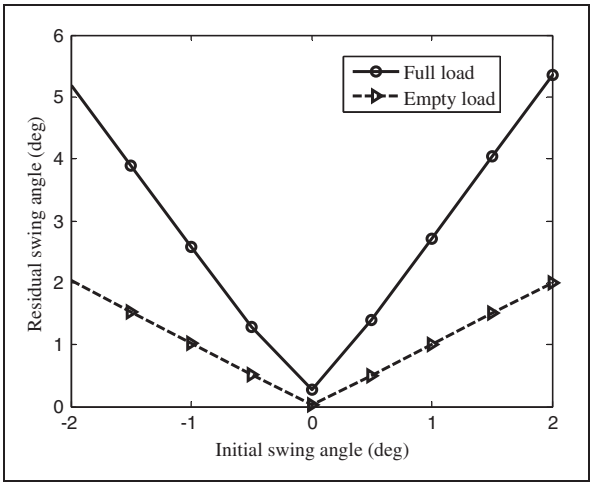

Figure 11. Curves of the residual swing angle varying with the initial swing angle.

of control parameters have a wide adaptive range for initial length of the rope and a narrow range for displacement of the trolley. Figure 11 indicates that the residual swing angle is sensitive to the initial swing angle, especially in full load path.

Conclusions

This paper proposes an IZV method of swing control of bridge-type grab ship unloader based on input-shaping method. A dynamic model of trolley–grab system considering damping and changing length of rope is built. Then an IZV method that uses the equivalent frequency and equivalent damping ratio to respond to system changes in rope length is presented and the optimal path planning is considered to avoid collision and improve efficiency. A numerical simulation of a case study is carried out to analyze the effects of the method proposed in this paper.

It was found that the max residual swing angle of the grab can be limited in a little range in ensuring the safety and the efficiency using this method to get optimal input commands. After that, the sensitivities of the max residual swing angle to the changes of some main designing parameters and operating parameters are analyzed, in which the unchangeable control parameters are used.

In addition, the results display that the residual swing angle is sensitive to the deviation of the center of gravity of the grab, the deviation of trolley's position, and the initial swing angle under the same control parameters, but insensitive to the damping coefficient, the time delay of the system, and the initial length deviation of the rope, which can help to select appropriate parameter values or adaptive range in an actual unloader. Because the center of gravity of the grab may be significant changes when the grab opens from full load to empty load, further research is needed to consider the effects according to 3D model.

This method is promising to extend to other situation, such as the swing control of container crane.

Declaration of Conflicting Interest

The author(s) declared no potential conflicts of interest with respect to the research, authorship, and/or publication of this article.

Funding

The author(s) disclosed receipt of the following financial support for the research, authorship, and/or publication of this article: This work is supported by the China Scholarship Council, the National Natural Science Foundation of China (Grant No. 51175395), and Wuhan Guide electric Co., Ltd.

References

1. Singhose W. Command shaping for flexible systems: a review of the first 50 years. *Int J Precis Eng Man* 2009; 10: 153–168.
2. Singer N, Singhose W and Kriikku E. An input shaping controller enabling cranes to move without sway. *Seventh topical meeting on robotics and remote systems*. Augusta: American Nuclear Society, 1997, pp.225–231.
3. Singhose W, Porter L and Seering W. Input shaped control of a planar gantry crane with hoisting. In: *1997 American control conference*, New Mexico, USA: IEEE Albuquerque, 1997, pp.97–100.
4. Singhose W, Porter L, Kenison M, et al. Effects of hoisting on the input shaping control of gantry cranes. *Control Eng Pract* 2000; 8: 1159–1165.
5. Hong KT, Huh CD and Hong KS. Command shaping control for limiting the transient sway angle of crane systems. *Int J Control Autom* 2003; 1: 43–53.
6. Blackburn D, Singhose W, Kitchen J, et al. Advanced command shaping algorithm for nonlinear tower crane dynamics. In: *Eighth international conference on motion and vibration control*, Daejeon, Korea: Korea Society of Mechanical Engineers, 2006, pp.860–865.
7. Blackburn D, Singhose W, Kitchen J, et al. Command shaping for nonlinear crane dynamics. *J Vib Control* 2010; 16: 477–501.
8. Khalid A, Frakes D, Huey J, et al. Human operator performance testing using an input-shaped bridge crane. *J Dyn Syst-T ASME* 2006; 128: 835–841.
9. Ngo QH, Nan Y and Hong KS. Command shaping for vibration reduction of container cranes. In: *Twelth IEEE international conference on control, automation and systems*, Jeju Island, Korea, 2012.
10. Veciana JM and Cardona S. Residual vibration reduction in low damping systems generation of regular piecewise algebraic polynomial inputs. *J Vibroeng* 2011; 13: 739–754.
11. Veciana JM and Cardona S. Residual vibration reduction in mechanical systems: a time-domain approach. *Int J Precis Eng Man* 2012; 13: 1327–1339.
12. Veciana JM, Cardona S and Català P. Minimizing residual vibrations for non-zero initial states: application to an emergency stop of a crane. *Int J Precis Eng Man* 2013; 14: 1901–1908.
13. Sorensen KL, Singhose W and Dickerson S. A controller enabling precise positioning and sway reduction in bridge and gantry cranes. *Control Eng Pract* 2007; 15: 825–837.
14. Stergiopoulos J and Tzes A. An adaptive input shaping technique for the suppression of payload swing in three-dimensional overhead cranes with hoisting mechanism. In: *Twelth IEEE international conference on emerging technologies and factory automation*, Patras, Greece: IEEE, 2007, pp.565–568.
15. Garrido S, Abderrahim M, Giménez A, et al. Anti-swinging input shaping control of an automatic construction crane. *IEEE T Autom Sci Eng* 2008; 5: 549–557.
16. Singhose W and Towell S. Double-pendulum gantry crane dynamics and control. In: *1998 IEEE international conference on control applications*, Trieste, Italy: IEEE, 1998, pp.1205–1209.
17. Singhose W, Kenison M and Kim D. Input shaping control of double-pendulum bridge crane oscillations. *J Dyn Syst-T ASME* 2008; 130: 034504.
18. Kim D and Singhose W. Performance studies of human operators driving double-pendulum bridge cranes. *Control Eng Pract* 2010; 18: 567–576.
19. Vaughan J, Kim D and Singhose W. Control of tower cranes with double-pendulum payload dynamics. *IEEE T Contr Syst T* 2010; 18: 1345–1358.
20. Masoud Z, Alhazza K, Abu-Nada E, et al. A hybrid command-shaper for double-pendulum overhead cranes. *J Vib Control* 2012; 20: 24–37.
21. Masoud ZN and Alhazza KA. Frequency-modulation input shaping control of double-pendulum overhead cranes. *J Dyn Syst-T ASME* 2014; 136: 021005.
22. Smith OJM. Posicast control of damped oscillatory systems. *Proc IRE* 1957; 45: 1249–1255.
23. Singer NC and Seering WP. Preshaping command inputs to reduce system vibration. *J Dyn Syst-T ASME* 1990; 112: 76–82.
24. Singhose W, Derezinski S and Singer N. Extra-insensitive shapers for controlling flexible spacecraft. *J Guid Control Dyn* 1996; 19: 385–391.
25. Singhose W, Seering W and Singer N. Input shaping for vibration reduction with specified insensitivity to modeling errors. *Japan-USA Symp Flexible Autom* 1996; 1: 307–313.
26. Singhose W and Pao L. A comparison of input shaping and time-optimal flexible-body control. *Control Eng Pract* 1997; 5: 459–467.
27. Vaughan J, Yano A and Singhose W. Comparison of robust input shapers. *J Sound Vib* 2008; 315: 797–815.
28. Vaughan J, Yano A and Singhose W. Performance comparison of robust negative input shapers. In: *2008 American control conference*, Seattle, Washington, USA: IEEE, 2008, pp.3257–3262.
29. Singhose W, Singer N and Seering W. Design and implementation of time-optimal negative input shapers. In: *ASME 1994 international mechanical engineering congress and exposition*, Chicago, Illinois, USA, 1994, pp.151–157.
30. Singhose W, Singer N and Seering W. Time-optimal negative input shapers. *J Dyn Syst-T ASME* 1997; 119: 198–205.
31. Sorensen K, Daftari A, Singhose W, et al. Negative input shaping: Eliminating overcurrenting and maximizing the command space. *J Dyn Syst-T ASME* 2008; 130: 061012.
32. Vaughan J, Yano A and Singhose W. Robust negative input shapers for vibration suppression. *J Dyn Syst-T ASME* 2009; 131: 031014.
33. Potter J, Singhose W and Costelloy M. Reducing swing of model helicopter sling load using input shaping. In: *Ninth IEEE international conference on control and automation*, Santiago, Chile, 2011, pp.348–353.
34. Hu Y, Wu B, Vaughan J, et al. Oscillation suppressing for an energy efficient bridge crane using input shaping. In: *Ninth IEEE Asian control conference*, Istanbul, Turkey, 2013, pp.1–5.
35. Lee HH. A new motion-planning scheme for overhead cranes with high-speed hoisting. *J Dyn Syst-T ASME* 2004; 126: 359–364.
36. Alhazza KA. Experimental and numerical validation on a continuous modulated wave-form command shaping control considering the effect of hoisting. In: *ASME 2013 International Design Engineering Technical Conferences (IDETC) and Computers and Information*

in Engineering Conference (CIE), Portland, USA: ASME, V07AT10A057, 2013.
37. Vazquez C, Collado J and Fridman L. On the second order sliding mode control of a parametrically excited overhead-crane. In: *2012 American control conference*, Montreal, QC, Canada: IEEE, 2012, pp.6288–6293.

Appendix

Notation

a_{G1}/a_{G2}	rated up/down acceleration
a_{Tj} (j=4)	accelerations of different stages in shaped speed curve of the trolley
A_i	amplitudes of the impulses
c	damping coefficient
f	friction on the trolley
F	drive force on the trolley
F_l	pull force of the rope
G	dissipation function
l	length of the rope
m	mass of the grab
M	mass of the trolley
O_1	position of the center of gravity of the trolley, the coordinate origin
O_2	coordinate of the grab
S_{OU}	distance between point O and point
t_i	time locations of the impulses
t_{Ge}	end time of lifting of the grab
t_{Gs}	start time of lifting of the grab
t_{Te}	end time of moving of the trolley
t_{Ts}	start time of moving of the trolley
t_{Tu}	time that the trolley reaches the point U
v_{Ge}	rated lift speed
v_m	velocity of the grab
v_M	velocity of the trolley
v_{Ti} (i=3)	velocities of different stages in shaped speed curve of the trolley
x	displacement of trolley
Δl	changing length of the rope
Δt_{Zk} (k=2)	delay times of different stages in shaped speed curve of the trolley
ζ	damping ratio
ζ_e	equivalent damping ratio
$\zeta_{\min}$	minimal damping ratio
$\zeta_{\max}$	maximal damping ratio
θ	swing angle of the grab
ω	natural frequency
ω_e	equivalent frequency
$\omega_{\min}$	minimal frequency
$\omega_{\max}$	maximal frequency